# Tumors of the Spine: When Can Biopsy Be Avoided?

Marc-André Weber, MD, MSc[1] Alberto Bazzocchi, MD, PhD[2] Iris-M. Nöbauer-Huhmann, MD[3]

[1] Institute of Diagnostic and Interventional Radiology, Pediatric Radiology and Neuroradiology, University Medical Center Rostock, Rostock, Germany
[2] Diagnostic and Interventional Radiology, The Rizzoli Orthopedic Institute, Bologna, Italy
[3] Department of Biomedical Imaging and Image Guided Therapy, Division of Neuroradiology and Musculoskeletal Radiology, Medical University of Vienna, Vienna, Austria

**Address for correspondence** Marc-André Weber, MD, MSc, Institute of Diagnostic and Interventional Radiology, Pediatric Radiology and Neuroradiology, University Medical Center Rostock, Ernst-Heydemann-Str. 6, 18057 Rostock, Germany (e-mail: marc-andre.weber@med.uni-rostock.de).

Semin Musculoskelet Radiol 2022;26:453–468.

## Abstract

Regarding osseous tumors of the spine, characteristic morphology is encountered in hemangioma of the vertebral body, osteoid osteoma (OO), osteochondroma, Paget's disease, and bone islands. In these cases, radiologic imaging can make a specific diagnosis and thereby avoid biopsy, especially when the radiologist has chosen the correct imaging modality to establish the diagnosis, such as thin-slice computed tomography in suspected OO. A benign lesion is suggested by a high amount of fat within the lesion, the lack of uptake of the contrast agent, and a homogeneous aspect without solid parts in a cystic tumor. Suspicion of malignancy should be raised in spinal lesions with a heterogeneous disordered matrix, distinct signal decrease in T1-weighted magnetic resonance imaging, blurred border, perilesional edema, cortex erosion, and a large soft tissue component. Biopsy is mandatory in presumed malignancy, such as any Lodwick grade II or III osteolytic lesion in the vertebral column. The radiologist plays a crucial role in determining the clinical pathway by choosing the imaging approach wisely, by narrowing the differential diagnosis list, and, when characteristic morphology is encountered, by avoiding unnecessary biopsies.

**Keywords**
- spine tumors
- biopsy
- magnetic resonance imaging
- patient management
- review

The most common benign bone tumor of the spine is hemangioma. Metastases, lymphoma, and multiple myeloma are the most frequent malignant lesions. Metastases, myeloma, and lymphoma generally present as multifocal lesions in the spine, thus making the diagnosis quite straightforward, along with the patient's clinical history.[1]

Imaging has a pivotal role in the detection and characterization of spinal bone tumors, especially using magnetic resonance imaging (MRI) and computed tomography (CT). In conjunction with the clinical history, imaging is generally used to differentiate benign from malignant lesions and narrow the list of differential diagnoses by searching for the usual signs of aggressiveness of the lesion itself, evaluating cortical destruction, neighboring bone, and periosteal reaction (e.g., by CT) or bone marrow edema and soft tissue extension (e.g., by MRI).[1] Moreover, MRI is indispensable to determine the extension and the relationship of the spinal bone tumor with the spinal canal and nerve roots, and thus determine the management plan.[2]

Furthermore, with the available more advanced imaging techniques, such as hybrid imaging, dynamic contrast-enhanced MRI, chemical shift and diffusion-weighted MRI, Dixon MR sequences, and dual-energy CT,[1] the differential diagnosis list may be narrowed to an extent that no biopsy is needed, for instance in vertebral hemangiomas, bone islands, and osteoid osteomas (OOs). However, because imaging features of benign and malignant spinal bone tumors may overlap, even when a multimodality imaging approach has

**Issue Theme** Spine Imaging; Guest Editors, Alberto Bazzocchi, MD, PhD and Giuseppe Guglielmi, MD


Thieme Medical Publishers, Inc., 333 Seventh Avenue, 18th Floor, New York, NY 10001, USA

**DOI** https://doi.org/10.1055/s-0042-1753506.
**ISSN** 1089-7860.

been sought and the diagnosis may remain uncertain, a bone biopsy should be performed to reach the final diagnosis.[1,3]

Of note, the final diagnosis can only be made when the biopsy is diagnostic, that is, it has yielded enough material for the pathologist to ensure an unequivocal diagnosis. In this respect, it is important to realize that the diagnostic yield (i.e., the percentage of biopsies that are considered diagnostic) of malignant bone tumors of the spine is significantly higher compared with the diagnostic yield of benign lesions, especially when they are cystic.[4] This could be due to the presence of more stromal tissue with fewer cellular components and higher cell heterogeneity without specific cellular morphology in benign lesions, compared with malignant ones that usually contain more consistent cells and stroma.[5] Therefore, the radiologist can influence patient management by ascertaining that a lesion is benign and thus prevent a possibly nondiagnostic biopsy.

This review article describes osseous tumors of the spine with characteristic morphology, such as hemangioma of the vertebral body, OO, osteochondroma, Paget's disease, and bone islands. In these cases, radiologic imaging can make a specific diagnosis and thereby avoid biopsy. Hence the radiologist has to choose wisely the specific imaging modality to make the diagnosis, for instance thin-slice CT in suspected OO. Therefore, so-called safety features of the entities are summarized.

Second, we address the imaging signs and techniques that help narrow the differential diagnosis, such as integration of diffusion-weighted imaging (DWI), dynamic contrast-enhanced MR imaging, Dixon-type and chemical shift imaging, to appreciate the fat content of a lesion or nuclear medicine techniques.

Third, we emphasize that biopsy is mandatory in unclear lesions or when histologic/immunohistologic and genetic analyses are needed to optimize therapy (such as in Ewing's sarcoma).

## Safety Features of Benign Spinal Lesions That Do Not Need Biopsy

### Hemangioma

Vertebral hemangioma is very common with a prevalence of 10 to 12% in adults. It is mostly discovered incidentally, with a reported prevalence ranging from 10% to 27% and related to increasing age. It is multiple in up to a third of patients.[2] Histologically, hemangiomas are a collection of thin-walled endothelial-lined blood vessels interspersed between nonvascular components, such as fat, muscle, fibrous tissue, or bone.[2] On CT, the hemangioma appears as a lesion that rarefies the bone with thickened vertical trabeculae, showing the typical pathognomonic "polka-dot sign" on axial images. Rarefied coarse trabeculae have a "corduroy pattern" on sagittal CT images.[6] On MRI, it generally shows high signal intensity on T1- and T2-weighted images with thickened hypointense trabeculae.

The so-called safety feature is the polka-dot aspect on thin-slice CT. Thus in atypical hemangiomas or even aggressive (also called compressive) hemangiomas of the vertebral body with less fat content and more vascular components, the additional use of CT to prove the polka-dot aspect can make a specific diagnosis (►**Fig. 1**). The keys to diagnosis in these cases with low adipocyte content is the wisely chosen CT as the only or the additional imaging modality to verify thickened and rarefied trabeculae,[6] so no biopsy is necessary in nearly all cases.

Laredo et al[7] demonstrated that vertebral hemangiomas with a higher fat content are generally quiescent lesions, whereas those with imaging features suggesting a higher vascular content are more likely to display active behavior and potentially evolve to compressive lesions. These "atypical" and "aggressive" vertebral hemangiomas are a radiologic challenge because they can mimic primary bony malignancies, focal bone marrow infiltration due to multiple myeloma, or metastases.[8]

As mentioned earlier, CT plays a central role in the work-up of atypical vertebral hemangiomas because it is the most appropriate modality to highlight the polka-dot appearance on axial CT images that is representative of them (►**Fig. 2**). The typical polka-dot sign as an expression of the thickened vertical trabeculae should always be sought, even in the more aggressive/compressive lesions, because it can guide the correct diagnosis.[8] In addition to imaging, the radiologist may look at clinical and laboratory data, when metastases or multiple myeloma is suspected, to identify a history of malignancy or a monoclonal gammopathy, elevated serum calcium levels, renal failure, or anemia.

In summary, biopsy can be avoided when the thickening of intralesional trabeculae is evidenced by CT in cases of equivocal MR features of atypical or aggressive hemangiomas. In doubtful cases, DWI, dynamic-contrast-enhanced MR imaging, and chemical shift MR imaging can be considered additional helpful tools.[1]

### Osteoid Osteoma of the Spine

Because 10% of all OOs are located in the spine, the key message here is to think of an OO when encountering a lytic lesion surrounded by a sclerotic osseous reaction located in the posterior elements of the thoracic and lumbar spine in a child or adolescent.[9,10] In our experience, the diagnosis is often delayed because the nidus (i.e., the tumor itself) may be hardly discernible when solely using MRI. The reactive edema surrounding the nidus may obscure visualization of the nidus that has a low to intermediate signal on T1-weighted images and an intermediate to high signal on T2-weighted images.[2]

Thus in case of suspicion, a thin-slice CT definitely helps identify the radiolucent vascular nidus with or without the intranidal calcification often associated with cortical thickening and bony sclerosis to establish the diagnosis (►**Fig. 3**).[2] In our centers, we use local ablative treatment options such as radiofrequency ablation (RFA) of the nidus without biopsy[9,10] when there is characteristic OO morphology in imaging, together with a typical clinical presentation. We share the prevailing opinion that a histologic confirmation is not necessary in the typical constellation of OO.[9,11] A vascular groove sign is a highly specific sign for distinguishing OOs from other radiolucent bone lesions on CT.[12]

 

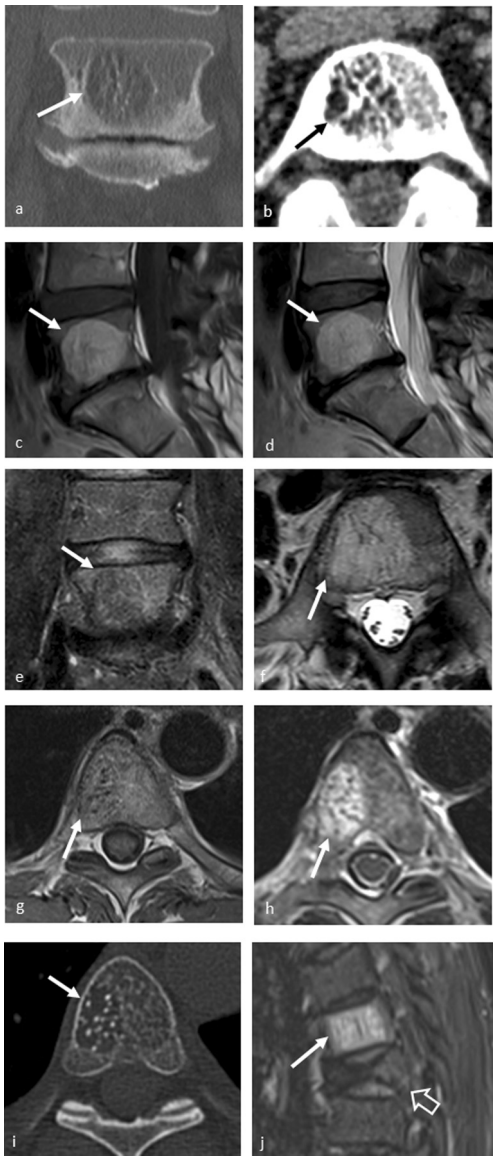

**Fig. 1** Vertebral hemangiomas (vascular malformations). Typical versus atypical vertebral hemangioma. (a–f) Typical (classic) hemangioma of the spine on computed tomography (CT) and magnetic resonance imaging (MRI) in a 47-year-old woman with severe degeneration at L5–S1 and incidental finding of a so-called typical fat-containing vascular malformation in L5. The CT shows coarse vertical trabeculation in the coronal reformation (a, arrow), polka dots, and some spoke-wheel appearance in the axial reformations, with fat best seen in (**b**) the soft tissue window. (**c**) MRI with sagittal T1-weighted sequence, (**d**) sagittal T2-weighted sequence, and (**e**) coronal short tau inversion (STIR) recovery, as well as (**f**) the axial T2-weighted sequence, confirm the fatty matrix of the hemangioma (arrows). (g–j) A 61-year-old woman with atypical vertebral hemangioma of T6 (arrows in **g–j**) and compression fracture of T7 (open arrow in **j**). (**g**) Axial T1-weighted sequence. (**h**) Axial T2-weighted sequence. (**i**) Axial CT. (**j**) Sagittal STIR. In contrast to classic vertebral hemangiomas, the atypical ones have less fatty and greater vascular content. Hence they appear iso- to hypointense on T1-weighted images due to low adipocyte content (g) and show very high signal intensity on T2-weighted and fluid-sensitive images (h, j) due to the prevalent vascular components. Within the hyperintense lesion, T1-weighted and T2-weighted images show punctuate and linear areas of iso- to hypointensity in the axial and sagittal plane, respectively, corresponding to thickened vertical trabeculae. (i) Axial CT reveals the typical polka-dot sign that supports the correct diagnosis. Thickened vertical trabeculae may be more difficult to see in atypical vertebral hemangiomas, but they are clearly evident here both on CT and MRI (arrows). This finding on CT and MR images should always be considered a key feature for the diagnosis.

**Fig. 2** Aggressive vertebral hemangioma (vascular malformation). Aggressive hemangioma of the vertebral body of L1 in a 34-year-old man with pain in both thighs and numbness of the dorsal left thigh. (**a**) Sagittal T2-weighted sequence. (**b**) Sagittal T1-weighted. (**c**) Axial T1-weighted. (**d**) Axial contrast-enhanced T1-weighted. (**e**) Computed tomography (CT) in coronal reformation. (**f**) CT in sagittal reformation. (**g**) Axial CT. (**h**) Selective angiography of the right L1 lumbar artery. (**i**) Status after embolization with coils and particles. (**j**) Lateral radiograph after decompressive laminectomy and partial resection of the vertebral body. This aggressive vertebral hemangioma was hypervascularized, and angiography demonstrates multiple blood pools within the vertebral body and had an epidural component (arrows) with draped curtain sign evident in (c) and (d). The hypervascularization of the L1 vertebral body via the L1 lumbar arteries on both sides was treated by coil embolization of the muscular branch of the right L1 artery and embolization with particles (size 500–700 µm) from both L1 arteries. After devascularization, partial resection of the L1 vertebral body, vertebral body replacement, and dorsal spondylodesis T11–L1 was performed. Histology revealed hemangioma without any signs of malignancy. These aggressive vertebral hemangiomas are a radiologic challenge because they can mimic primary bony malignancies, focal bone marrow infiltration due to multiple myeloma, or metastases. As in this case, CT plays a central role in the work-up because it is the most appropriate imaging modality to highlight the polka-dot appearance representative of them. The typical polka-dot sign should always be sought on axial CT images (g) because it can support the correct diagnosis. As in this case, surgery is indicated in cases of rapid or progressive neurologic symptoms with neural element decompression and spine stabilization as the main goals. Preoperative embolization can help manage the intraoperative bleeding of these hypervascular lesions.

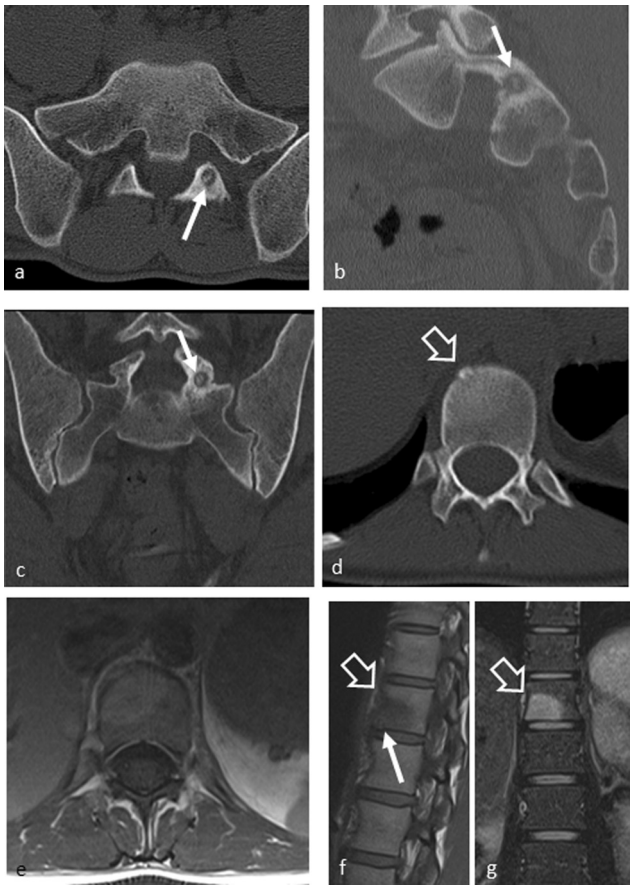


**Fig. 3** Osteoid osteoma (OO) of the spine. (**a–c**) A 38-year-old man with OO (arrows) in the lamina of the first sacral vertebra. The centrally calcified osteolytic nidus (arrows) is surrounded by a zone of bony sclerosis. (d, e) A 22-year-old woman with night pain responding to salicylates. (**d**) The OO of 5 mm in diameter presents with a nearly completely calcified nidus at the anterior and inferior border of the 12th thoracic vertebra adjacent to the inferior vena cava (open arrow) in the axial computed tomography (CT). There is also subtle perifocal sclerosis visible in the cancellous bone of T12. In the unenhanced magnetic resonance imaging scans, the nidus is not visible. (**e**) Axial T1-weighted sequence. (**f**) Sagittal T1-weighted. (**g**) Coronal short tau inversion recovery. In the sagittal T1-weighted sequence, with knowledge of the CT, a subtle lesion may be found (f, arrow). The perifocal bone marrow edema is clearly visible in T12 (f, g, open arrows).

Dynamic contrast-enhanced MRI was shown to identify the nidus more clearly than unenhanced MRI or static postcontrast MR sequences. Most OOs show arterial phase enhancement and rapid partial washout as a result of the hypervascularity of the nidus.[13] In a recent trans-European multicenter study with a large cohort of 77 patients with spinal OO and 10 patients with spinal osteoblastoma (OB), RFA proved to be a safe and efficient method to treat spinal OO and OB with technical and clinical success rates of 94.8% and 89.6%, respectively, for spinal OO and 90.0% and 90.0%, respectively, for spinal OB.[10]

Other local ablative techniques were also described as efficient in diagnosing OO, such as RFA or other techniques like interstitial laser ablation,[14] microwave ablation,[15] cryoablation,[16] or high-intensity focused ultrasound ablation.[17] For an overview of available thermal ablation procedures, see Dalili et al.[18] Thus, in our opinion, a typical OO in the spine can be treated without prior biopsy with local ablative techniques. Regarding solitary true bone tumors of the vertebral column (i.e., no mimickers and secondary bone tumors), OO is the only entity that permits skipping a biopsy. All other primary bone tumors of the spine have to be ultimately diagnosed with an intraprocedural biopsy and any specimens obtained during the procedure sent for histologic evaluation to obtain a definitive diagnosis.

This protocol is necessary to achieve best practices and optimize patient care. Biopsies are performed before planning therapeutic procedures in all "indeterminate," "suspicious," "probably malignant," and/or "definitely malignant" tumors for histologic diagnosis and grading.[18] The results should be discussed in multidisciplinary tumor board meetings consisting of at least a tumor or spine surgeon, a pathologist, and an experienced musculoskeletal radiologist before any subsequent intervention.[19,20]

## Osteoblastoma of the Spine

OB is a good example of an indeterminate lesion. An OO > 15 mm is called an OB.[21] This entity is four times less frequent than OO, appears more expansive, and has fewer sclerotic borders. OB in 30 to 40% of all cases affects the vertebral column and in 85% originates from the posterior elements, with 42% extending into the vertebral body.[2] In addition, OB may show more aggressive imaging (and histologic) features than OO (in these cases, naming it as a giant OO is misleading). Malignant transformation into osteosarcoma is rare but possible. Consequently, histologic sampling is mandatory in all cases.[2,22]

The most common appearance of spinal OB is an expansile lesion with a prominent sclerotic rim and multiple small calcifications (►**Fig. 4**). The more aggressive type also demonstrates bone destruction and paravertebral extension.[2] As with OO, the radiologic examination of choice is CT, showing the multifocal matrix calcifications (as opposed to central ones in OO), the sclerotic margin, expansile bone remodeling, or a thin osseous shell around its margins, whereas MRI better depicts the surrounding soft tissue involvement.[2] The radiologist can only avoid an unnecessary biopsy by exactly measuring the nidus size on thin-slice CT data sets with multiplanar reconstructions because per definition, a nidus size < 1.5 cm in maximum diameter turns an OB into an OO that needs no biopsy before the intervention.

## Osteochondroma of the Spine

Osteochondromas of the spine are rare and have a predilection for males and the cervical spine.[2] The radiologist can make a probable diagnosis of a cartilaginous exostosis of the vertebral column by demonstrating a continuous trabecular bone from the vertebra to the exostosis. In typical cases with a thin cartilage cap, no underlying hereditary multiple exostoses disease, and no symptoms, biopsy can be avoided and a watchful waiting concept applied by using whole-body MRI, for example.[23]

 


**Fig. 4** Osteoblastoma (OB) of the spine. (a, b) OB with typical giant osteoid osteoma (OO) appearance in a 14-year-old boy. (**a**) Coronal computed tomography (CT) reformation. (**b**) Axial T2-weighted sequence. The OB within the left lamina of the fifth lumbar vertebra has centrally accented matrix calcifications similar to an OO (open arrows in **a, b**). (c–f) OB in a 20-year-old man does not have a giant OO appearance but presents as an expansive lesion with a prominent sclerotic rim and multiple small calcifications. Moreover, this more aggressive OB type also demonstrates bone destruction and paravertebral extension (d, arrow) (c) Axial CT in soft tissue, (d) bone kernel. (**e**) Sagittal T2-weighted sequence. (**f**) Axial contrast-enhanced fat-saturated T1-weighted sequence. Here the space-occupying effect is much more pronounced when compared with the first case, and there is widening of the right neuroforamen and perilesional reaction of the soft tissues (f, arrow). The thin osseous shell around its margins is best demonstrated on CT (d, arrow). Magnetic resonance imaging better depicts the surrounding soft tissue involvement (f).

Osteochondromas of the spine are often difficult to detect on radiographs because of the complex osseous anatomy and frequent small size of the lesions. The lesions are best evaluated by thin-section multiplanar CT images to detect the pathognomonic continuity of the marrow and cortical portions of the carrying bone into the exostosis.[2] The hyaline cartilage cap is usually apparent with MRI and typically has high signal intensity on T2-weighted sequences. The key role of the radiologist is to measure the thickness of the cartilage cap accurately because exostoses with a thick cartilage cap have the potential of malignant degeneration into a low-grade chondrosarcoma. A malignant transformation is more likely if the thickness of the cartilage cap is $\geq 1$ cm (►**Fig. 5**), if the exostosis is near the trunk, in cases with growth of the

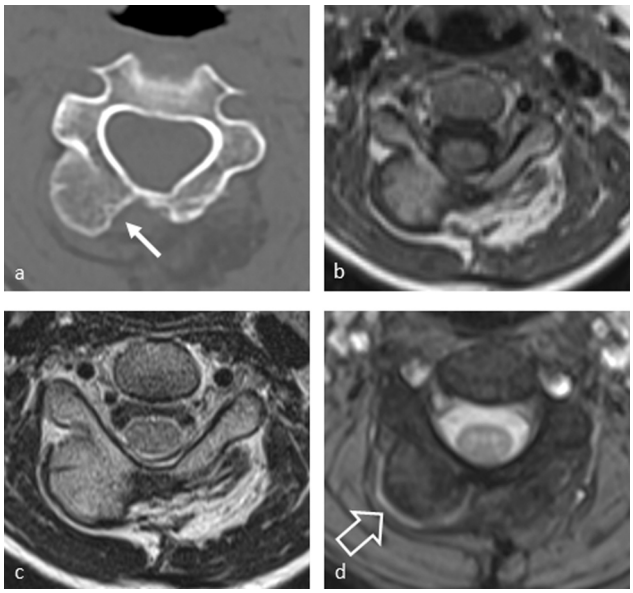


**Fig. 5** Osteochondroma (cartilaginous exostosis) of the vertebral column. A 12-year-old girl with a painless hard (bonelike) swelling of the neck. (**a**) Axial computed tomography (CT) reformation shows an exophytic lesion with a broad base and typical cortical and marrow continuity of the lesion and parent bone (arrow). On magnetic resonance imaging, (**b**) axial T1-weighted sequence, (**c**) axial T2-weighted, and (**d**) T2* Multiple Echo Data Image Combination (MEDIC) sequences, the interface between the lesion and the parental bone is confirmed, along with a very small cartilaginous cap of the osteochondroma (d, open arrow). The patient's medical history documented an osteochondroma adjacent to the lesion that was removed a few years earlier.

cartilage cap, especially after the 20th year of life, and in cases of hereditary multiple exostoses.[24,25]

Hereditary multiple exostoses is an autosomal dominant disorder, in which spinal exostoses are present in up to 9% of patients and in which 3 to 5% of tumors develop into chondrosarcoma. In all suspected cases of secondary chondrosarcoma, complete resection is necessary. Spinal chondrosarcomas are frequently localized (40–90%) in the posterior elements of the spine (most commonly the thoracic segments) and typically evolve in older patients with a male-to-female ratio of 2 to 4:1.[2] Most spinal chondrosarcomas are histologically low-grade lesions and typically have a slow growth rate. Signs of the chondroid matrix are typical popcorn calcifications and ring-and-arc nodules pattern best visualized on CT.[2] They need histologic grading for treatment planning; hence biopsy is mandatory.

## Aneurysmal Bone Cyst of the Spine

An aneurysmal bone cyst (ABC) can be located in the vertebral column in 13 to 30% of all cases and typically affects the dorsal elements, but 75 to 90% of cases extend into the vertebral body although centered posteriorly. ABCs make up 5% of all benign bone tumors and tumor-like lesions and affect mainly (75%) young people $< 20$ years of age, causing minor pain and occasional swelling.[2,26] According to the World Health Organization, ABC is classified as a destructive, expansive benign neoplasia. Multiple cavities, filled with unclotted blood and surrounded by septa, are typical. In a

 


**Fig. 6** Aneurysmal bone cyst (ABC) of the spine. (a–c) A girl 13.7 years of age with pain at the thoracic vertebral column for 3 weeks. She had received physiotherapy. She presented with distally accentuated paraparesis for 3 days; walking without help was no longer possible. Clinical examination revealed tenderness at T6–T8 and numbness below T10. (**a**) Axial computed tomography (CT) shows the lytic expansive soap-bubble appearance of the ABC at T7 (arrow). (**b**) Axial contrast-enhanced fat-saturated T1-weighted sequence illustrates septal enhancement (open arrow) and the (**c**) sagittal T2-weighted sequence demonstrates fluid-fluid levels (open arrow). Open surgery with decompression because of the acute transverse spinal cord syndrome was performed, together with posterior spondylodesis. Localization, age, and the fluid-fluid-levels, as well as the ballooned cortices in imaging, point to an ABC. (d–f) An 11-year-old girl with ABC of the third lumbar vertebra. (**d**) CT in sagittal and (**e**) coronal reformation demonstrate the typical soap-bubble appearance and the expansive growth, as well as the thinned cortex or neocortex formation (arrows). (**f**) The axial T2-weighted sequence shows typical fluid-fluid levels (open arrow).

true ABC, no atypical cells are found, but secondary ABCs exist in relation with other tumors such as giant cell tumors.[24,26]

Highly suspicious for ABC on MRI and CT are the cystic appearance, internal septations with a multiloculated appearance, frequent involvement of posterior elements, and intralesional fluid-fluid levels due to hemorrhage (►**Fig. 6**). However, the latter is not pathognomonic because fluid-fluid levels can also be observed in malignant lesions such as telangiectatic osteosarcoma.[25] Thus before surgery, biopsy sampling should be performed, ideally focused on any strongly contrast-enhancing solid part. Importantly, the crucial role of the radiologist is to detect any solid component within an ABC, which would be the biopsy target!

Fluid-fluid levels on cross-sectional imaging should be avoided during biopsy for two reasons. First, if there are no solid components, CT and ultrasonography-guided core needle bone biopsies have a low diagnostic rate in large cystic bone tumors without a soft tissue component, so other methods of management like open resection should be considered in such cases.[27] Second, the primary tumor that has caused a secondary ABC will be missed because a biopsy will not harbor diagnostic tissue of the primary tumor when only directed to the fluid-fluid levels of the ABC.

In summary, in suspected ABC the radiologist has to scrutinize the entire lesion to identify any solid, contrast-enhancing part, which is the biopsy target. Watchful waiting can be discussed with asymptomatic patients whose dedicated imaging showed no solid parts.

## Bone Islands

A bone island, or enostosis, is defined as a focus of compact bone within the spongiosa, probably representing a developmental error of endochondral ossification: misplaced hamartomatous cortical bone.[28,29] Bone islands are asymptomatic lesions that are discovered incidentally in patients of all ages. They are not true neoplasms; that is, they represent a developmental abnormality and consist of dense compact bone within spongiosa.

Radiography and CT demonstrate round osteoblastic lesions with a brush border at their periphery. Enostoses have low signal intensity on T1- and T2-weighted MR sequences (►**Fig. 7**). They may show activity at bone scintigraphy in $< 10\%$ of cases, and most lesions remain stable. Enostoses are mostly $< 2$ cm but may vary in size, and some giant enostoses have been reported in the literature.[6] Typically asymptomatic, the lesion is usually an incidental finding, with a preference for the pelvis, femur, and other long bones, although it may be found anywhere in the skeleton, including the spine, where it is frequently located between T1 and T7 and L2 and L3. The primary alternative in the differential diagnosis is osteoblastic metastasis.[28,29]

When can biopsy be avoided? A bone island can be virtually diagnosed based on its characteristic clinical and radiologic features. Thus the radiologist should establish the diagnosis and avoid an unnecessary biopsy.[2] However, biopsy may be considered if there is an increase in size. Bone islands are typically solitary; however, multiple lesions are related to osteopoikilosis.[2]

Keys to diagnosis are a homogeneous high density within cancellous bone, spiculated margins along trabeculae, that is, radiating bony streaks (brush border or thorny radiation), low signal intensity on T1- and T2-weighted sequences, and no uptake on nuclear bone scans.[6] Osteoblastic metastases, in contrast, typically show tracer uptake in bone scintigraphy and have signs of aggressiveness such as bone destruction.[6] The diagnosis of spinal bone islands can be more challenging when the imaging examinations has been performed because of staging purposes in case of underlying cancer or when no precedent imaging is available (►**Fig. 7**). Here,

 

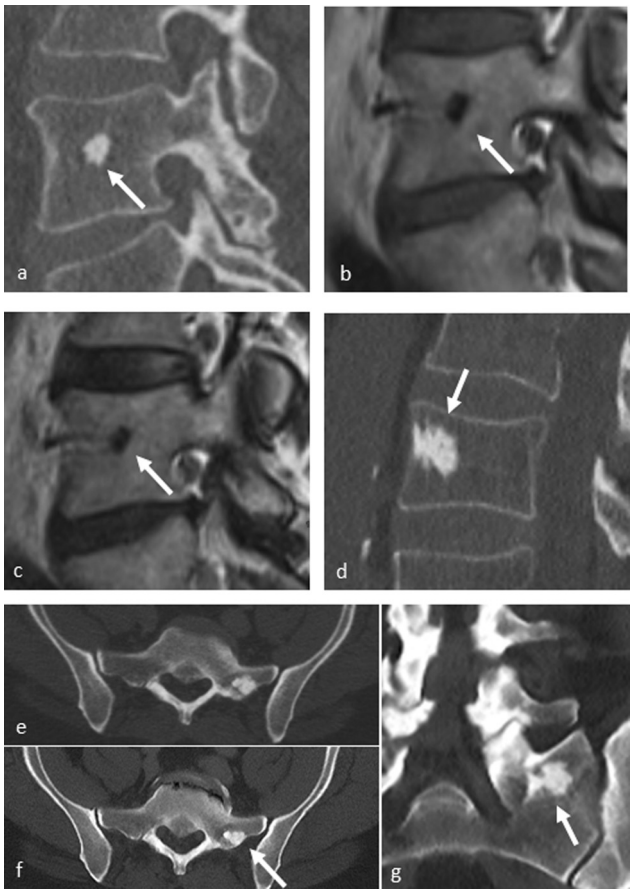


**Fig. 7** Bone island, or enostosis, of the vertebral column. (a–c) A 57-year-old-woman with a vertebral bone island in the L4 vertebral body. (**a**) Computed tomography (CT) shows an incidental finding of a small sclerotic lesion (arrow) with feet-like extensions, typical for a bone island. The lesion is hypointense on all sequences (arrows), without surrounding reaction, in the (**b**) sagittal T1-weighted and (**c**) T2-weighted sequences. **(d)** This vertebral bone island in the vertebral body of L3 in a 67-year-old patient has the typical spiculated margins along trabeculae (arrow), that is, radiating bony streaks (also called brush border or thorny radiation). These radiating bony streaks, or "pseudopodia," aligned with the axis of the host bone's trabeculae that merge with the latter in a feathered or brush-like fashion, are distinguishing features. Also, the typical orientation with the long axis of the bone, parallel to the cortex is observed. (e–g) CT was performed in a 51-year-old-man for staging after ultrasonography found suspicious liver lesions. (**e**) There is a bone island within the massa lateralis of the left sacral bone. Now 4.5 years later, the lesion is absolutely stable: (**f**) Axial CT (arrows). (**g**) Coronal reformation. The liver lesions turned out to be hemangiomas. The bone islands are homogeneously dense, and there is a sclerotic ovoid focus on CT within cancellous bone.

the radiologist can really play a decisive role in patient management by identifying the keys to the diagnosis of a bone island.

## Presumed Malignancy

The radiologist plays a crucial role in the clinical pathway because his or her role is to choose the imaging approach wisely, to narrow the differential diagnosis list and to perform the image-guided biopsy after interdisciplinary case discussion. Hence we as radiologists have to identify the imaging setting. Here are some examples:

I. No underlying malignancy => solitary lesion => may be OO, vertebral hemangioma, bone island? => diagnosis with imaging alone possible!
II. No underlying malignancy => solitary lesion => not unequivocally benign => may be primary tumor of the spine => histologic verification mandatory!
III. No underlying malignancy => more than one lesion => may be vertebral hemangiomas or bone islands? => diagnosis with imaging alone possible!
IV. Known neoplasia => more than one lesion => may be vertebral hemangiomas or bone islands? => diagnosis with imaging alone possible (radiologist is decision maker)!
V. Known neoplasia => any number of lesions that are not unequivocally benign => may be primary or secondary tumor of the spine => histologic verification or short-term follow-up mandatory!
VI. Known neoplasia => multiple aggressive lesions => metastases most likely => biopsy only if treatment scheme would be altered.
VII. Known neoplasia under follow-up => imaging is sufficient to detect progression, stable disease, or remission. Biopsy is usually not necessary. In our practice, MRI is performed in all patients to assess the response to the intervention and/or plan further treatments.[18,30,31] In addition to MRI, to merely estimate the response to therapy and to detect progression or local or distant recurrence early on, hybrid imaging techniques, such as positron emission tomography (PET)/CT and PET/MRI, are sufficient and highly specific for this purpose.[31]

Primary tumors of the spine, for instance, giant cell tumors, chordoma, chondrosarcoma, and osteosarcoma (►**Fig. 8**), are uncommon and represent < 5% of all bone neoplasms when compared with secondary metastatic disease, multiple myeloma, and lymphoma.[2] Thus we omit an extensive description of these entities here but focus on the settings when the radiologist can justify to an interdisciplinary case board that a biopsy can be avoided. Of note, as a rule of thumb, histologic verification or confirmation of a suspected diagnosis by short-term follow-up should be sought in any doubtful case regarding the benignity of the lesion or when metastases or myeloma lesions are very probable and no histologic verification is necessary to optimize therapy.

### Ewing's Sarcoma and Lymphoma

Lesions for which therapy depends on confirmation of histology results should be biopsied.[32] Hence in every case of presumed malignant bone lesions of the vertebral column, a biopsy is mandatory to reach a definitive histologic genetic diagnosis that will affect the treatment schemes. Examples for this scenario may be Ewing's sarcoma and all other histologically similar tumors with a broad differential diagnosis list. Conventional radiography reveals an aggressive osteolytic lesion with a wide zone of transition and with a moth-eaten or permeative pattern in most cases.[33]

 

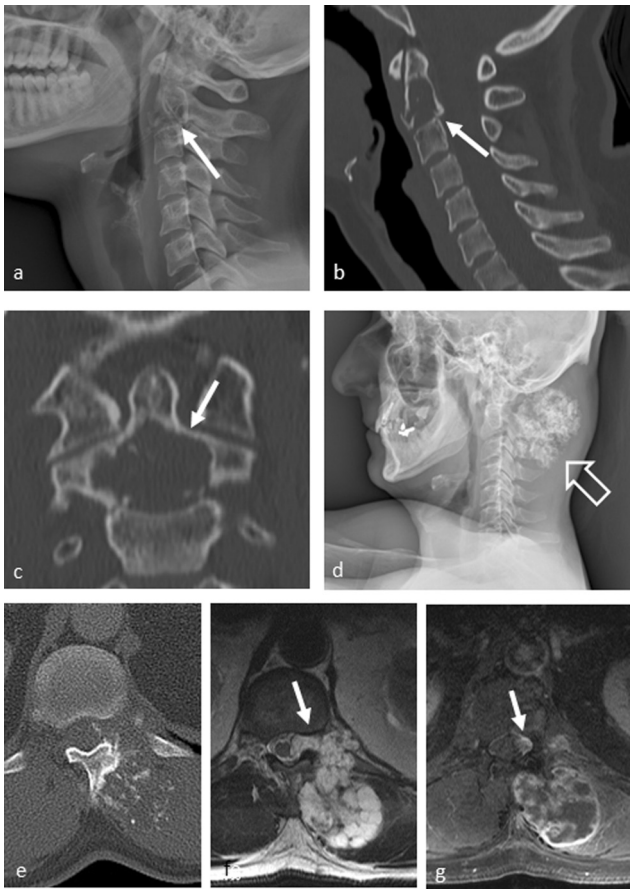


**Fig. 8** Spinal lesions that definitely warrant biopsy. Osteosarcoma of the dentoid process of the axis in a 32-year-old woman. (**a**) Lateral radiograph. (**b, c**) Computed tomography (CT) in sagittal and coronal reformation presenting as a lytic cortex-penetrating lesion (arrows in **a–c**). (**d**) Chondrosarcoma (open arrow) arising from the posterior elements of C2 and C3 in a 42-year-old man presents with popcorn calcifications of the tumor matrix (lateral radiograph). (e–g) Chondrosarcoma in a 64-year-old man presenting with diffuse low back pain accentuated at the level of the left kidney and hardening of the left erector spinae muscle at T11–L1 but no paresis and no loss of sensation at clinical examination. (**e**) Axial CT performed to rule out renal calculus shows the destructive mass with invasion of the spinal canal and with flocculent, snowflake matrix calcifications. The invasion through the left T12 neuroforamen is best seen on magnetic resonance imaging (arrows in **f, g**). (**f**) The signal intensity of the chondroid matrix is high on the T2-weighted sequence and shows peripheral contrast enhancement on (**g**) the axial fat-suppressed contrast-enhanced T1-weighted sequence.

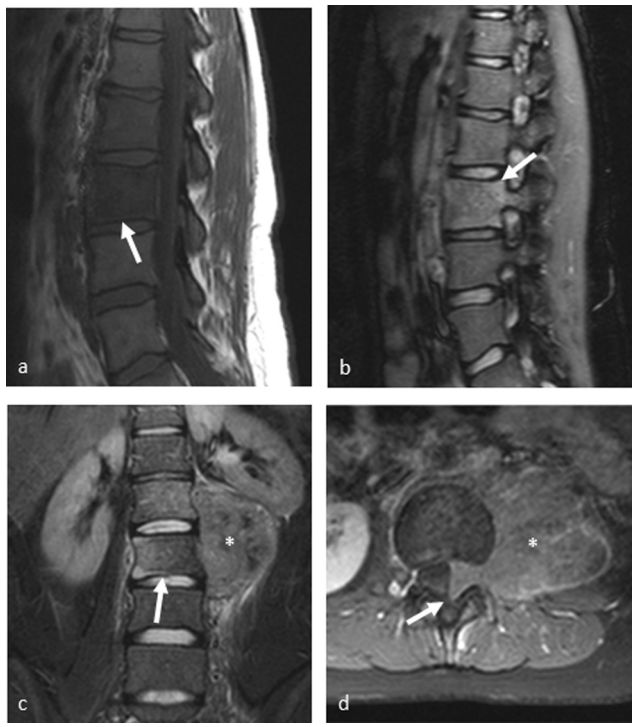


**Fig. 9** Ewing's sarcoma of the vertebral column. The Ewing's sarcoma of the third lumbar vertebra (arrows) in a 18-year-old woman presents with a large soft tissue component on the left paravertebral side (asterisk) and infiltration through the left neuroforamen (arrow). Nearly the entire third lumbar vertebra is affected by the tumor. **(a)** Sagittal T1-weighted sequence. **(b)** Sagittal short tau inversion recovery (STIR). **(c)** Coronal STIR. **(d)** Axial contrast-enhanced fatsaturated T1-weighted sequence.

Ewing's sarcoma is a rare, highly malignant anaplastic stem cell tumor of neuroectodermal origin, also classified as round cell sarcoma, to which the primitive neuroectodermal tumors also belong. It mainly arises from the bone.[34] About up to 15% of all Ewing's sarcomas are localized in the vertebral column with the lumbar spine and the sacrum most commonly affected; the location of Ewing's sarcoma tends to follow the distribution of red marrow. Metastases of Ewing's sarcoma affecting the vertebral column are more common than a primary Ewing's sarcoma of the spine.[24] At histology, the typical appearance at hematoxylin-eosin staining is small blue round cells without any matrix formation. The list of differential diagnosis is long, substantiating the crucial role of histologic verification. In general, all other tumors consisting of small round blue cells may have a similar imaging aspect. The main differential diagnoses comprise osteolytic osteosarcoma and small-cell osteosarcoma in children and adolescents, osteomyelitis in all age groups, and non-Hodgkin's lymphoma in adulthood.[35] In children, unifocal Langerhans cell histiocytosis is another differential. In the spine, Ewing's sarcoma may mimic spondylitis because of its high signal intensity in T2-weighted images,[25,36] whereas in the rare case of sacroiliac joint involvement, it should be distinguished from septic sacroiliitis.[37]

MRI is the method of choice for local staging because it demonstrates the true tumor extension (►**Fig. 9**).[38] The standard of care for Ewing's sarcoma states that after completion of imaging, the final diagnosis will be verified at histology and by genetic markers from biopsy material. That biopsy should be performed in a dedicated sarcoma treatment center.[19] Moreover, in Ewing's sarcoma, histologic sampling is mandatory because the treatment is interdisciplinary and consists of induction chemotherapy and local therapy with subsequent chemotherapy and/or radiation therapy within multicentric study protocols. In these protocols, neoadjuvant chemotherapy with histopathologic assessment of tumor response to induction neoadjuvant chemotherapy, followed by local therapy, such as surgical tumor resection and reconstruction, and optionally followed by radiation therapy is recommended.[39] Hence biopsy is

 

mandatory whenever Ewing's sarcoma is suspected. Biopsy is required in all cases of presumed malignancy, such as any Lodwick grade II or III osteolytic lesion in the vertebral column.

The same rule applies to primary and secondary osseous lymphomas. Lymphomas are a heterogeneous group of primary neoplasms of the lymphoid tissue and may be classified as Hodgkin's disease or non-Hodgkin's lymphoma. Primary osseous lymphoma must be distinguished from a secondary bone involvement by lymphomas arising from inner organs or lymph nodes.[38] Thus for the correct categorization of an osseous lymphoma, the radiologist's role is to exclude simultaneous extraosseous manifestations of lymphoma at other locations.

Primary osseous lymphomas are most commonly highly malignant B-cell lymphomas.[40] About 50% of all primary osseous lymphomas are localized within the skeleton of the trunk and skull. Secondary lymphomas also favor the spine and should be distinguished from primary multifocal lymphoma.[41] Like Ewing's sarcoma, primary osseous lymphomas have an indistinct tumor margin and show an invasive diffuse growth pattern. The pattern of extensive marrow disease and surrounding soft tissue masses but without extensive cortical destruction was reported nearly exclusively in round cell tumors such as primary lymphomas of the bone, multiple myeloma, and Ewing's sarcoma.[42] At hematoxylin-eosin histologic staining, the tumor stroma consists of diffuse round cell infiltrates, and this aspect resembles the appearance of Ewing's sarcoma. On radiographs or CT, primary lymphomas of the bone may appear as solitary osteolytic or multiple osteolytic lesions with an aggressive destruction pattern. Similar to Ewing's sarcoma, the permeative and moth-eaten destructive pattern indicates the presence of a tumor consisting of small or round cells.

MRI, as in Ewing's sarcoma, is the method of choice for the work-up of symptomatic areas, especially in case of suspected compression of the spinal cord or spinal nerves. The signal behavior itself is nonspecific and may also show a diffuse or focal replacement of normal bone marrow, as could be seen in multiple myeloma. As in Ewing's sarcoma, the differential diagnosis list is long, and the patient's age is the crucial parameter. Typical differential diagnoses are Ewing's sarcoma, unifocal Langerhans cell histiocytosis, and osteolytic osteosarcoma in young patients. In older adults, typical differential diagnoses comprise metastases (e.g., small-cell tumors such as bronchial carcinoma), fibrosarcoma, and osteomyelitis.

In summary, as in Ewing's sarcoma for verification of the final diagnosis, biopsy sampling and imaging correlation is always mandatory.[38] Although unfortunately, skeletal lymphomas had the highest percentage of unsuccessful biopsies (22%) in a series of 963 CT-guided core needle biopsies, compared with primary bone tumors, metastases, and myelomas.[43] Hence in osseous lymphomas, a disease-specific imaging biomarker is of utmost importance.

## Plasma Cell Disorders

The vertebral column is mostly affected in multiple myeloma. Solid myeloma nodules destroy the bone, and on CT multiple lytic lesions without any reactive zone or only a faint reactive zone may be seen in the multifocal disease pattern. About 70% of patients with multiple myeloma are $>60$ years of age. A soft tissue mass is an indicator of a poor prognosis. If the radiologist encounters multiple lytic lesions in an adult $>40$ years, he or she should think of metastases or multiple myeloma.[44] Thus an "image wisely" approach is to look at a nuclear bone scan that may have been performed earlier. A negative bone scan and no primary tumor as the cause of metastases in the medical history hint at multiple myeloma. MRI is the best imaging modality to prove bone marrow involvement, which is T1-weighted hypointense and hyperintense on fat-saturated T2-weighted sequences.[45] The bone marrow infiltration may show a diffuse, multifocal, or "salt-and-pepper" pattern; plasmacytoma is the denominator of the single lesion.

In addition to imaging, the radiologist may examine clinical and laboratory data when multiple myeloma is suspected to identify a history of malignancy or a monoclonal gammopathy, elevated serum calcium levels, renal failure, or anemia. These CRAB (calcium elevation, renal insufficiency, anemia, and bone lesions) criteria identify symptomatic multiple myeloma in contrast to disease stages without end-organ damage, such as smoldering multiple myeloma and monoclonal gammopathy of undetermined significance.[44] The radiologist can only avoid unnecessary biopsies when he or she identifies multiple lesions.

However, despite being one disease, monoclonal plasma cell disorders show marked heterogeneity regarding genomics, phenotype, and prognosis.[46] In multiple myeloma, plasma cell clones may have a different genetic architecture in a single patient,[47] and therefore clonal heterogeneity can only be identified by taking several biopsy samples from different lesions. However, even in patients with a solitary plasmacytoma in the spine, the radiologist can help avoid biopsy in selected cases by identifying a "mini-brain sign," an expansile lesion within the spine characteristic of plasmacytoma (►**Fig. 10**).[48] Axial T2-weighted MR sequences typically show abnormal high signal intensity throughout the vertebral body and linear low signal intensity resembling sulci of the brain. These linear low-signal-intensity areas represent cortical thickening caused by compensatory hypertrophy of remaining trabecula. Radiologists should note this characteristic because biopsy can be avoided in patients with this appearance. This sign has been described as sufficiently pathognomonic to obviate biopsy and start treatment.[48]

## Metastases

Metastatic bone disease is the most common malignant bone lesion in adults. Approximately 40 to 70% of all bone metastases occur in the vertebral column, most often in the thoracic spine.[30,49] In 10% of patients, the neoplastic origin is unknown. Metastases may also appear as solitary osteolytic spinal lesions, but usually they are multiple and tend to show a wide zone of transition, ill-defined margins, and frequent vertebral collapse, similar to myelomatous locations in the spine.[1]

 

**Fig. 10** Plasmacytoma of the spine. A 60-year-old man who had thoracic pain for 1 month when coughing and recurrent episodes of night sweats for several years. (**a**) Axial computed tomography (CT). (**b**) CT in sagittal reformation. (**c**) Sagittal T1-weighted sequence. (**d**) Sagittal T2-weighted sequence. (**e, f**) Axial contrast-enhanced T1-weighted sequence. In this case of plasmacytoma of T5, the axial magnetic resonance imaging (MRI) implies a "mini-brain" appearance that has been reported to be characteristic. Arrows in the CT images point at the compensatory cortical thickening and hypertrophy of remaining trabecula that appear as linear low-signal-intensity areas on MRI resembling sulci of the brain (e, f, arrows).

**Fig. 11** Metastatic-induced pathologic vertebral fractures versus osteoporotic fractures of the spine. A 65-year-old woman with pathologic fracture of L2 because of vertebral metastasis of an adenocarcinoma of the corpus uteri. (**a**) Sagittal T1-weighted sequence. (**b**) Sagittal short tau inversion recovery (STIR). (**c**) Coronal STIR. (**d**) Axial T2-weighted sequence. (**e**) Computed tomography (CT) in sagittal reformation. The following signs favor a pathologic fracture: convex posterior border of the vertebral body (b, arrow), the replacement of the fatty marrow of the L2 vertebral body (a, arrow), the paraspinal soft tissue mass (c, d, open arrows), and the inhomogeneous bone structure on CT with osteosclerotic areas of L2 in comparison with L3 (e). (**f**) A 46-year-old woman (sagittal STIR) with osteoporotic fractures of T11 and L1 presenting with linear subtle edema along the upper end plates of T11 and L1 (arrows). Moreover, the concave posterior borders of the vertebral bodies make an osteoporotic fracture more likely than a pathologic fracture. (**g**) A 70-year-old woman with osteoporotic fracture of L3. (**f**) Sagittal T1-weighted sequence. (**g**) Sagittal STIR. (**h**) CT in sagittal reformation. The sagittal T1-weighted MR image (g) shows the compression fractures of L3 with normal residual bone marrow signal intensity in the vertebral body (arrow) and retropulsion of a bone fragment at the posterior portion of the vertebral body. There is also an intravertebral fluid sign (h, arrow) and (**i**) intravertebral vacuum phenomenon (arrow) that suggest a benign osteoporotic fracture.

Biopsy can be avoided in cases of known primary tumor and multiple bone lesions that fulfill the imaging criteria of metastases during the follow-up of bone metastases under therapy. In addition, imaging, especially MRI, can help differentiate osteoporotic from metastatic spinal fractures, for instance the posterior border of the vertebral body, the presence or absence of a "fluid sign," and the presence or absence of soft tissue masses (►**Fig. 11**).[50–53] Because osseous infection can mimic a bone tumor and metastasis, owing to the associated bony destruction and infiltration into the surrounding soft tissues, MRI can help with the differential diagnosis by identifying the preservation of the end plates and intervertebral disks in metastatic bone diseases.

Biopsy can be thus avoided only in cases of known (multifocal) bone metastases when the tissue sampling of an individual lesion is not necessary. On the other side, indications for further histologic verification of a presumed spine metastases include[32] (1) cases of more than one primary tumor, (2) when a primary tumor is not verified (cancer of unknown primary [CUP] syndrome), (3) solitary aggressive bone lesion, and finally (4) for the proposal of targeted/precision therapies, such as the identification of new targets for treatment (as already described in the setting of clonal heterogeneity of multiple myeloma bone lesions). As a rule of thumb, biopsy cannot be avoided in malignant

lesions like metastases in case of unknown primary and in all cases when genetic testing and grading influences modern treatment schemes in the setup of precision medicine.[30]

### Lesion Size

Biopsy can be avoided and a follow-up examination within 6 weeks or 3 months may be reasonable (in an "image wisely" setting) when the lesion is small, for instance $< 5$ mm. In this situation, all available imaging biomarkers and biopsy may not be diagnostic. For instance, the diagnostic yield of CT-guided biopsy of bone tumors is significantly lower for lesions $< 20$ mm compared with bigger lesions. Several articles showed that the size of the lesion is important for the success of the imaging-guided biopsy of skeletal tumors because of the amount of the obtained material and the possibility of sampling error. The optimal size of the lesion for successful imaging-guided biopsy should be $\geq 20$ mm, according to the authors.[4,54–57]

## Non-neoplastic Diseases

Several developmental, inflammatory, metabolic, focal reactive, and posttraumatic entities may mimic both benign and malignant tumors of the spine.[2] Examples are Paget's disease and fibrous dysplasia as tumor-like lesions that may also involve the spine as well as the appendicular skeleton.

### Paget's Disease of the Spine

Osteodystrophia deformans, or Paget's disease, leads to focal excessive bone resorption with subsequent overwhelming new formation of woven bone. The disease progresses in three stages that continuously merge into one another. The osteolytic phase is characterized by circumscribed, in the long bones with often wedge- or flame-shaped osteolysis pointing toward the diaphysis. Then the compensatory osteoblastic response begins, and the lytic areas of the radiograph become radiodense in the older portions of the lesions. This mixed phase is accompanied by a coarsening of the trabecular structure and the cortical bone. The third stage of Paget's disease is the osteosclerotic phase when new bone formation occurs with accompanying expansion of the affected bone. In the late stages of the disease, the entire lesion is radiodense. In 65 to 90% of patients, a polyostotic pattern is present, and in the osteolytic and mixed stage of the disease, a nuclear bone scan typically demonstrates avid tracer uptake of the affected bones.[6] In contrast to Paget's disease, bone metastases typically show cortical destruction.[6]

The identification of Paget's disease can be challenging, especially when the imaging examinations were performed for staging purposes in the case of underlying cancer or when no precedent imaging is available. Thus the radiologist plays a key role in decision making and patient management. He or she must direct the diagnosis to Paget's disease and recommend additional imaging, such as bone scintigraphy, to strengthen the diagnosis. In the osteolytic and mixed stages of Paget's disease, there is significant uptake in skeletal scintigraphy while uptake in the osteosclerotic phase may be unremarkable. The radiologic features parallel the histologic changes, and in many cases the diagnosis can be made solely on the basis of plain radiographs.

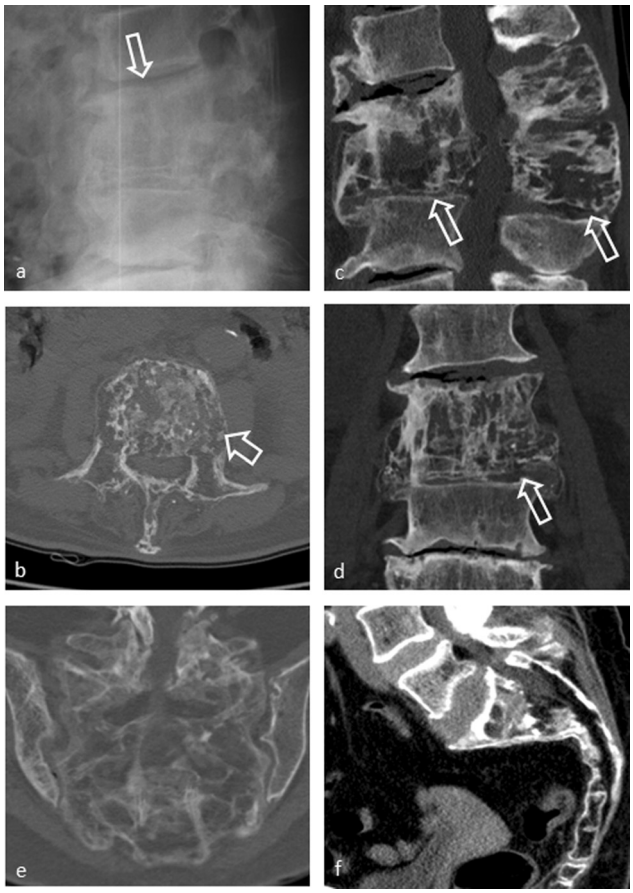


**Fig. 12** Paget's disease of the spine. (a–d) A 78-year-old man with affection of the third and fourth vertebral body including the posterior appendicular structures. (**a**) Lateral radiograph of the lumbar spine. (**b**) Axial computed tomography (CT). (**c**) CT in sagittal reformation. (**d**) CT in coronal reformation. Coarsening of the trabecular structure and the cortical bone, as well as expansion of the affected bone, is clearly demonstrated (open arrows). (e, f) A 67-year-old woman with Paget's disease. (**e**) CT with coronal reformation, bone window. (**f**) CT with sagittal reformation, soft tissue window. There is a typical appearance of Paget's disease with remodeling of the sacral bone, sclerosis, which is most marked at the periphery and relatively lucent center, due to atrophy of the spongiosa.

Paget's disease is usually encountered in its late (radiodense) phase. Distinctive radiographic features of later stages of Paget's disease include coarsening of trabeculae, blurring of the cortical-medullary junction, narrowing of the medullary canal, and thickening or enlargement of the bone (►**Fig. 12**). This combination of features leads to radiodense bones. In addition to radiodensity, bone enlargement is another highly suggestive feature that is caused, in part, by periosteal new bone deposition. However, the earliest radiographic pattern, corresponding to the initial wave of osteoclastic resorption, is radiolucency. Because osteosarcoma may be associated with Paget's disease,[2,24] the radiologist should recommend biopsy in any cases of aggressiveness that do not fit one of the three stages of Paget's disease.

 

### Fibrous Dysplasia of the Spine

Fibrous dysplasia is a hereditary disorder in which normal bone marrow is replaced by fibro-osseous tissue and results from a mutation in the *GNAS-1* gene. In half of the cases, the disease manifests before the age of 20, in 75% before the age of 30 years. A distinction is made between mono-ostotic, which accounts for ~ 70% of all cases, and polyostotic forms. In the mono-ostotic form, the ribs are most frequently affected, followed by the proximal femora. The vertebral column is an uncommon presentation of the mono-ostotic form; the lumbar spine is affected in 14% of cases in the polyostotic form.[58,59]

The radiographic presentation of fibrous dysplasia depends primarily on the coexistence of fibrous and osseous components, with a purely fibrous structure forming geographic osteolysis. Fibrous dysplasia may have a ground-glass appearance as the initially lytic matrix calcifies. This rather pathognomonic finding is best seen on CT. The MRI signal in fibrous dysplasia depends on the amount of calcification, ossification, and fibrous tissue.[2] Thus MRI shows a T1-weighted isointense lesion whose T2-weighted signal characteristics can vary from isointense to strongly hyperintense due to the inhomogeneous stroma (►**Fig. 13**). The affected bones can also expand. The new inferior bone formed during the fibrous dysplasia often leads to deformities and then the characteristic shepherd's crook deformity, a coxa vara deformity, in the area of the proximal femora. The radiologist should raise the suspicion of fibrous dysplasia and recommend CT to demonstrate the typical ground-glass like internal structure of the vertebral lesion, which may show an increase in volume, typically without a periosteal reaction.[58,59] A biopsy is often not useful due to the very heterogeneous structure. However, if there is the slightest doubt about the benignity of a fibrous lesion, an en bloc resection should be performed for histologic confirmation.


**Fig. 13** Fibrous dysplasia of the vertebral column. A 33-year-old woman with fibrous dysplasia of C2 (open arrows). (**a**) Sagittal T2-weighted sequence. (**b**) Sagittal short tau inversion recovery. (**c**) Computed tomography (CT) in sagittal reformation. A 43-year-old woman with fibrous dysplasia of T10–T11 and paraspinal extension. (**d**) Axial CT. An 43-year-old woman with fibrous dysplasia (arrow) of L1. (**e**) Axial CT in a 18-year-old man with fibrous dysplasia of L1. (**f**) Axial CT in a 58-year-old woman. The manifestations of spinal fibrous dysplasia have these characteristics in common: expansile lesions, ground-glass opacity on CT, sclerotic rims, and no obvious soft tissue masses. Fibrous dysplasia may present as an expansile lytic lesion (e), if the matrix has not calcified. Sclerotic rim formation may be subtle (d) or more pronounced, as in (f). (**g**) Fibrous dysplasia of C7 in a 51-year-old woman. Axial CT in bone window. The lesion appears inhomogeneous, with lytic and more sclerotic areas, with minor areas of typical ground-glass appearance; the lesion is slightly expansile, with a thin neocortex.

### Infection of the Spine

Infection should always be considered in the differential diagnosis of tumors of the vertebral column, so biopsy material should be sent for both microbiological and histopathologic assessment.[19] By using DWI to detect restricted diffusion within the abscess cavity in cases of osteomyelitis and spondylodiskitis, MRI can narrow the differential diagnosis list.[60] Other criteria in favor of infectious spondylodiskitis are as follows (the sensitivity of the diagnostic sign is given in parentheses)[61]: disk hypointensity on T1-weighted (30%), disk hyperintensity on T2-weighted sequences (93%), decreased disk height (53%), contrast enhancement of disk (95%), erosion or destruction of at least one vertebral end plate on T1-weighted sequences (84%), and paraspinal/epidural inflammation (98%).

Hence the radiologist often encounters spinal infections in routine clinical practice, and when typical MRI features are present, the diagnosis is relatively straightforward, all the more so if the clinical and laboratory findings agree with the radiologic findings.[60,62] In many cases, the radiologist can make the correct diagnosis and thereby avoid a diskovertebral biopsy. These biopsies may be technically challenging and are also associated with a risk of negative results.[60,63] In case of inflammatory infiltration of the paravertebral space, the rate of successful pathogen detection in suspected spondylodiskitis by CT-guided biopsy is substantially higher.[64] Echinococcal infection may be presumed if hydatic cysts are

 

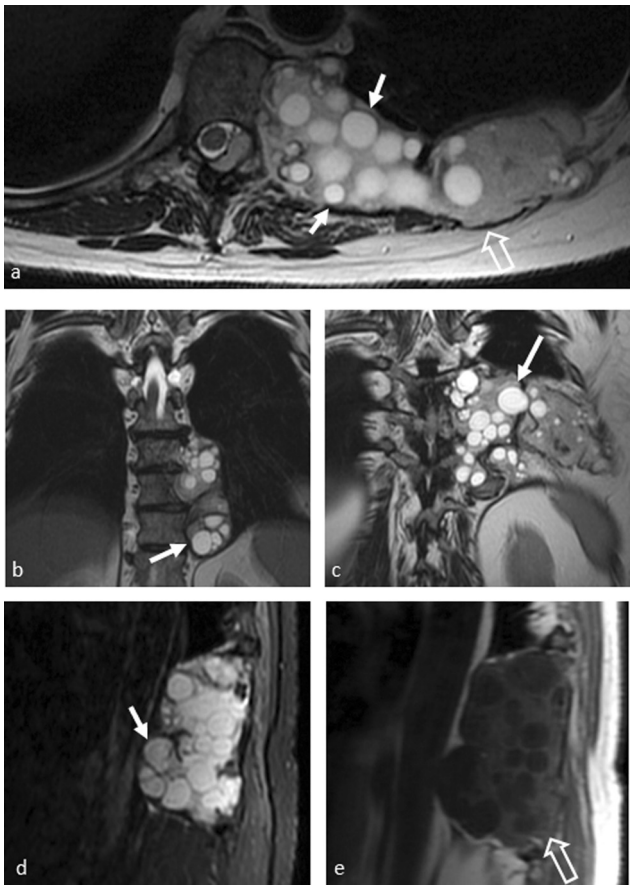


**Fig. 14** Echinococcosis (hydatid disease). A 55-year-old woman with hydatid disease of the thoracic spine. (**a**) Axial T2-weighted sequence. (**b, c**) Coronal T2-weighted sequences. (**d**) Sagittal short tau inversion recovery. (**e**) Sagittal T1-weighted sequence. Hints for echinococcal infection are the presence of multiple cystic lesions (arrows) in a mass lesion (open arrow).

encountered at the vertebral column.[24] They present with multiseptated lesions with minimal enhancement (►**Fig. 14**). Biopsy should be avoided because cyst rupture may cause anaphylaxis. The radiologist should raise the suspicion of echinococcal infection, and then a specific blood test should be performed to establish the diagnosis.

## Miscellaneous/Rare Differential Diagnoses

In addition to bone islands, two rare entities may mimic osteoplastic bone metastases. Hibernomas are rare benign tumors composed of variable quantities of brown fat. All studied cases of hibernomas of the vertebral column were asymptomatic and had sclerotic lesions of the axial skeleton. In all cases, the lesions were considered unusual, and the radiologic differential diagnosis in particular included hemangioma, bone island, benign notochordal cell lesion (BNCL), and metastasis. The typical MRI behavior is as follows: T1-weighted hypointense to subcutaneous fat and hyperintense to skeletal muscle, T2-weighted hyperintense with high signal rim, and in 60% peripheral or homogeneous contrast enhancement.[65] These lesions have largely presented as an incidental finding in asymptomatic middle-aged and older adults that on plain radiographs and CT are sclerotic and mostly in the axial skeleton. The keys to diagnosis are sclerotic lesions typically $< 2$ cm, minimal or prominent uptake on nuclear bone scan, T1-weighted hypointense sequences, and no aggressive appearance. Hence the radiologist here has the key role to clarify the benign nature of these lesions by ruling out signs of aggressiveness.

The same applies to BNCLs that are also called giant (vertebral) notochordal rest or benign notochordal cell tumor.[66–68] The notochord is an embryonic tissue that induces the development of the vertebral column in fetal life, and it completely disappears to form the nucleus pulposus of the intervertebral disk. BNCLs are usually confined to the vertebral body. They may not be visualized on plain film and are mildly osteosclerotic on CT. They have poorly defined margins due to the intervening residual bone trabeculae. They are "cold" on nuclear bone scan. They are iso- or hypointense on T1-weighted images and hyperintense on T2-weighted images. They typically do not enhance with intravenous contrast (►**Fig. 15**). The key role of the radiologist is to discriminate the benign entities from chordomas. The most significant discriminators between BNCLs and chordomas (►**Fig. 15**) are the presence or absence of extraosseous components in lesions (BNCLs are confined to the vertebral body), of bone destruction on CT or conventional tomography (BNCLs show no bone destruction), and contrast enhancement on T1-weighted MRI (BNCLs typically show no contrast enhancement). In summary, the lack of progression at follow-up, bone destruction, or soft tissue extension are important imaging criteria that suggest a radiologic diagnosis of a BNCL, again pointing out the key role of the radiologist in the decision-making process for optimal patient care.

Finally, cystic angiomatosis or systemic lymphangiomatosis may mimic osteolytic metastases. These two terms have been used interchangeably. The exact etiology is unknown, but the formation of cystic lymphangiomas is thought to be due to sequestration of lymphatic vessels during embryogenesis. It is considered a malformation of the lymphatic system rather than a neoplasm. Cystic angiomatosis is a rare disorder characterized by a diffuse or multifocal involvement of bones, parenchymal organs, or soft tissues by cystic vascular spaces.[69–71] Several organ systems may be affected: bone, lung, pleura, spleen, liver, kidney, colon, small intestine, mesentery, body wall, skin, supraclavicular soft tissues, neck, and axilla. Histologically, the dilated vascular spaces resemble lymphangiomas, with large endothelial-lined spaces. Therefore, several authors prefer the term *lymphangiomatosis*; however, it may be difficult to establish whether the vascular lesions are blood vessels or true lymphatics. Moreover, the involvement of both lymphatic and vascular channels is frequent, and different organs may contain different types of lesions. The disease occurs mainly in children or adolescents. Multiple variably sized osteolytic lesions are seen throughout the skeleton, and the radiologist should raise the suspicion, if these findings coincide: the absence of both cortical destruction and periosteal reaction, incidental painless bone lesions, density $\sim$ 5 to 8 HU, as well as the multifocal involvement of bones, parenchymal organs, and/or soft tissues.

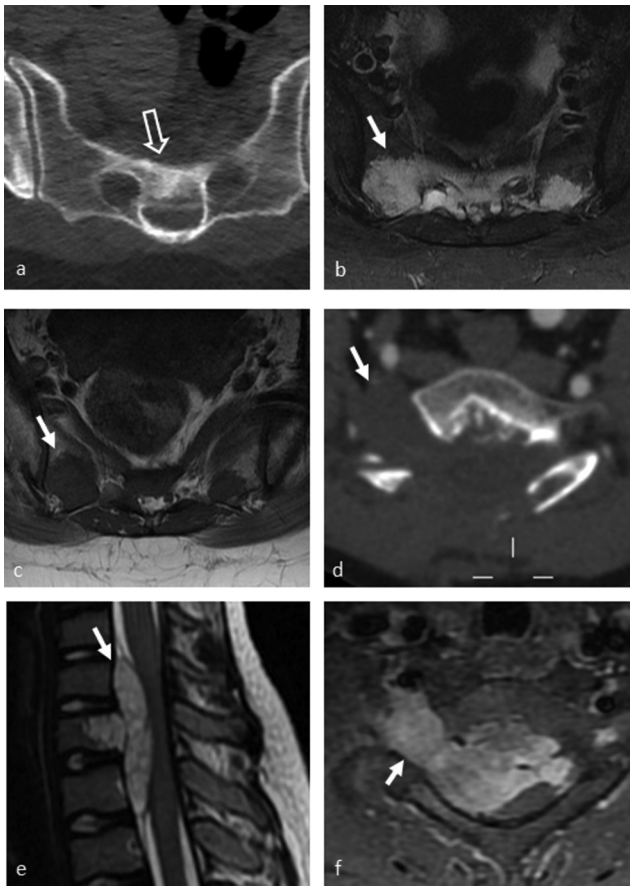


**Fig. 15** Benign notochord cell tumor (benign notochord cell lesion) in the sacrum of a 56-year-old woman. (**a**) Axial computed tomography (CT). (**b**) Axial short tau inversion recovery. (**c**) Axial T1-weighted sequence. The T2-weighted hyperintense, T1-weighted-hypointense entity is confined to the bone (arrows in **b, c**) and mildly osteosclerotic on CT (open arrow in **a**). The key role of the radiologist is to discriminate this benign entity form chordomas. The presence of extraosseous components (arrows in **d–f**) and bone destruction on CT suggest chordoma in this 11-year-old boy with chordoma arising from the seventh cervical vertebral body. (**d**) Axial CT. (**e**) Sagittal T2-weighted sequence. (**f**) Fat-saturated contrast-enhanced axial T1-weighted sequence.

## Summary

Characteristic morphology is encountered in hemangioma of the vertebral body, OO, osteochondroma, Paget's disease, and bone islands. Suggested characteristics of a rather benign lesion are a high amount of fat within the lesion, lack of contrast agent uptake, and a homogeneous aspect without solid parts in the case of a cystic tumor. Suspicion of malignancy should be raised in spinal lesions with heterogeneous disordered matrix, distinct signal decrease in T1-weighted MRI (many cells), blurred border, perilesional edema, cortex erosion, and with a large soft tissue component (fast growth). Biopsy is mandatory in presumed malignancy, such as any Lodwick grade II or III osteolytic lesion in the vertebral column. In general, permeative and moth-eaten destructive patterns of the bone indicate a possible small or round cell tumor. Thus histologic confirmation should always be sought in presumed malignant tumors such as Ewing's sarcoma and lymphoma that have also been described as the chameleon of the bone tumors, given their diverse imaging appearance. Because especially at the vertebral column, due to projection effects, bone neoplasms with remarkably normal-appearing radiographs may show distinct abnormalities on MRI or bone scintigraphy, further assessment with a more sensitive modality, such as MRI, is essential in patients with persisting symptoms but negative radiographs ("image wisely"). However, in suspected OO and OB, thin-slice CT is the modality of choice.

Conflict of Interest
None declared.

## References

1 Albano D, Messina C, Gitto S, Papakonstantinou O, Sconfienza LM. Differential diagnosis of spine tumors: my favorite mistake. Semin Musculoskelet Radiol 2019;23(01):26–35
2 Orguc S, Arkun R. Primary tumors of the spine. Semin Musculoskelet Radiol 2014;18(03):280–299
3 Thawait SK, Marcus MA, Morrison WB, Klufas RA, Eng J, Carrino JA. Research synthesis: what is the diagnostic performance of magnetic resonance imaging to discriminate benign from malignant vertebral compression fractures? Systematic review and meta-analysis. Spine 2012;37(12): E736–E744
4 Rimondi E, Rossi G, Bartalena T, et al. Percutaneous CT-guided biopsy of the musculoskeletal system: results of 2027 cases. Eur J Radiol 2011;77(01):34–42
5 Nouh MR, Abu Shady HM. Initial CT-guided needle biopsy of extremity skeletal lesions: diagnostic performance and experience of a tertiary musculoskeletal center. Eur J Radiol 2014;83 (02):360–365
6 Wünnemann F, Rehnitz C, Weber MA. Incidental findings in musculoskeletal radiology. [in German]. Radiologe 2017;57 (04):286–295
7 Laredo JD, Assouline E, Gelbert F, Wybier M, Merland JJ, Tubiana JM. Vertebral hemangiomas: fat content as a sign of aggressiveness. Radiology 1990;177(02):467–472
8 Gaudino S, Martucci M, Colantonio R, et al. A systematic approach to vertebral hemangioma. Skeletal Radiol 2015;44(01):25–36
9 Weber MA, Sprengel SD, Omlor GW, et al. Clinical long-term outcome, technical success, and cost analysis of radiofrequency ablation for the treatment of osteoblastomas and spinal osteoid osteomas in comparison to open surgical resection. Skeletal Radiol 2015;44(07):981–993
10 Beyer T, van Rijswijk CSP, Villagrán JM, et al. European multicentre study on technical success and long-term clinical outcome of radiofrequency ablation for the treatment of spinal osteoid osteomas and osteoblastomas. Neuroradiology 2019;61(08):935–942
11 Rehnitz C, Sprengel SD, Lehner B, et al. CT-guided radiofrequency ablation of osteoid osteoma and osteoblastoma: clinical success and long-term follow up in 77 patients. Eur J Radiol 2012;81(11): 3426–3434
12 Liu PT, Kujak JL, Roberts CC, de Chadarevian JP. The vascular groove sign: a new CT finding associated with osteoid osteomas. AJR Am J Roentgenol 2011;196(01):168–173
13 Davies M, Cassar-Pullicino VN, Davies AM, McCall IW, Tyrrell PN. The diagnostic accuracy of MR imaging in osteoid osteoma. Skeletal Radiol 2002;31(10):559–569
14 Gangi A, Alizadeh H, Wong L, Buy X, Dietemann JL, Roy C. Osteoid osteoma: percutaneous laser ablation and follow-up in 114 patients. Radiology 2007;242(01):293–301
15 Kostrzewa M, Henzler T, Schoenberg SO, Diehl SJ, Rathmann N. Clinical and quantitative MRI perfusion analysis of osteoid

 

osteomas before and after microwave ablation. Anticancer Res 2019;39(06):3053–3057
16 Cazzato RL, Auloge P, Dalili D, et al. Percutaneous image-guided cryoablation of osteoblastoma. AJR Am J Roentgenol 2019;213 (05):1157–1162
17 Napoli A, Bazzocchi A, Scipione R, et al. Noninvasive therapy for osteoid osteoma: a prospective developmental study with MR imaging-guided high-intensity focused ultrasound. Radiology 2017;285(01):186–196
18 Dalili D, Isaac A, Bazzocchi A, et al. Interventional techniques for bone and musculoskeletal soft tissue tumors: current practices and future directions—Part I. Ablation. Semin Musculoskelet Radiol 2020;24(06):692–709
19 Lalam R, Bloem JL, Noebauer-Huhmann IM, et al. ESSR Consensus document for detection, characterisation, and referral pathway for tumors and tumorlike lesions of bone. Semin Musculoskelet Radiol 2017;21(05):630–647
20 Cazzato RL, Garnon J, De Marini P, et al. French multidisciplinary approach for the treatment of MSK tumors. Semin Musculoskelet Radiol 2020;24(03):310–322
21 Lucas DR. Osteoblastoma. Arch Pathol Lab Med 2010;134(10): 1460–1466
22 Papaioannou G, Sebire NJ, McHugh K. Imaging of the unusual pediatric 'blastomas.'. Cancer Imaging 2009;9:1–11
23 Jurik AG, Jørgensen PH, Mortensen MM. Whole-body MRI in assessing malignant transformation in multiple hereditary exostoses and enchondromatosis: audit results and literature review. Skeletal Radiol 2020;49(01):115–124
24 Rodallec MH, Feydy A, Larousserie F, et al. Diagnostic imaging of solitary tumors of the spine: what to do and say. Radiographics 2008;28(04):1019–1041
25 Kloth JK, Wolf M, Rehnitz C, Lehner B, Wiedenhöfer B, Weber MA. Radiological diagnostics of spinal tumors. Part 1: general tumor diagnostics and special diagnostics of extradural tumors. [in German]. Orthopade 2012;41(08):595–607
26 Murphey MD, Andrews CL, Flemming DJ, Temple HT, Smith WS, Smirniotopoulos JG. From the archives of the AFIP. Primary tumors of the spine: radiologic pathologic correlation. Radiographics 1996;16(05):1131–1158
27 Jakanani GC, Saifuddin A. Percutaneous image-guided needle biopsy of rib lesions: a retrospective study of diagnostic outcome in 51 cases. Skeletal Radiol 2013;42(01):85–90
28 Greenspan A. Bone island (enostosis): current concept—a review. Skeletal Radiol 1995;24(02):111–115
29 Greenspan A, Klein MJ. Giant bone island. Skeletal Radiol 1996;25 (01):67–69
30 Kintzelé L, Weber MA. Imaging diagnostics in bone metastases. [in German]. Radiologe 2017;57(02):113–128
31 Isaac A, Lecouvet F, Dalili D, et al. Detection and characterization of musculoskeletal cancer using whole body magnetic resonance imaging. Semin Musculoskelet Radiol 2020;24(06):726–750
32 Isaac A, Dalili D, Dalili D, Weber MA. State-of-the-art imaging for diagnosis of metastatic bone disease. Radiologe 2020;60 (Suppl 1):1–16
33 Murphey MD, Senchak LT, Mambalam PK, Logie CI, Klassen-Fischer MK, Kransdorf MJ. From the radiologic pathology archives: Ewing sarcoma family of tumors: radiologic-pathologic correlation. Radiographics 2013;33(03):803–831
34 Freyschmidt J, Ostertag H. Ewing's sarcoma, fibrogenic tumors, giant cell tumor, hemangioma of bone: radiology and pathology. [in German]. Radiologe 2016;56(06):520–535
35 McCarville MB, Chen JY, Coleman JL, et al. Distinguishing osteomyelitis from Ewing sarcoma on radiography and MRI. AJR Am J Roentgenol 2015;205(03):640–650; quiz 651
36 Ilaslan H, Sundaram M, Unni KK, Dekutoski MB. Primary Ewing's sarcoma of the vertebral column. Skeletal Radiol 2004;33(09): 506–513
37 Jordanov MI, Block JJ, Gonzalez AL, Green NE. Transarticular spread of Ewing sarcoma mimicking septic arthritis. Pediatr Radiol 2009;39(04):381–384
38 Weber MA, Papakonstantinou O, Nikodinovska VV, Vanhoenacker FM. Ewing's sarcoma and primary osseous lymphoma: spectrum of imaging appearances. Semin Musculoskelet Radiol 2019;23 (01):36–57
39 AWMF guideline: Ewing's sarcoma (in children and adolescents) of the German Society of Pediatric and Adolescent Medicine (DGKJ). Accessed May 31, 2022 at: https://www.awmf.org/uploads/tx_szleitlinien/025-006l_S1_Ewing-Sarkom-Kinder_-Jugendliche_2022-02_01.pdf
40 Ludwig K. Musculoskeletal lymphomas. [in German]. Radiologe 2002;42(12):988–992
41 Navarro SM, Matcuk GR, Patel DB, et al. Musculoskeletal imaging findings of hematologic malignancies. Radiographics 2017;37 (03):881–900
42 Krishnan A, Shirkhoda A, Tehranzadeh J, Armin AR, Irwin R, Les K. Primary bone lymphoma: radiographic-MR imaging correlation. Radiographics 2003;23(06):1371–1383; discussion 1384–1387
43 Chang CY, Huang AJ, Bredella MA, et al. Percutaneous CT-guided needle biopsies of musculoskeletal tumors: a 5-year analysis of non-diagnostic biopsies. Skeletal Radiol 2015;44(12):1795–1803
44 Weber MA, Baur-Melnyk A. Radiological diagnosis of multiple myeloma: Role of imaging and the current S3 guideline. [in German]. Radiologe 2022;62(01):35–43
45 Wennmann M, Kintzelé L, Piraud M, et al. Volumetry based biomarker speed of growth: Quantifying the change of total tumor volume in whole-body magnetic resonance imaging over time improves risk stratification of smoldering multiple myeloma patients. Oncotarget 2018;9(38):25254–25264
46 Wennmann M, Hielscher T, Kintzelé L, et al. Analyzing longitudinal wb-MRI data and clinical course in a cohort of former smoldering multiple myeloma patients: connections between MRI findings and clinical progression patterns. Cancers (Basel) 2021;13(05):961
47 Rasche L, Chavan SS, Stephens OW, et al. Spatial genomic heterogeneity in multiple myeloma revealed by multi-region sequencing. Nat Commun 2017;8(01):268
48 Major NM, Helms CA, Richardson WJ. The "mini brain": plasmacytoma in a vertebral body on MR imaging. AJR Am J Roentgenol 2000;175(01):261–263
49 Andreula C, Murrone M, Algra PR. Metastatic disease of the spine. In: Goethem JWM, Hauwe L, Parizel PM, eds. Spinal Imaging. Berlin/Heidelberg, Germany: Springer; 2007:461–474
50 Jung HS, Jee WH, McCauley TR, Ha KY, Choi KH. Discrimination of metastatic from acute osteoporotic compression spinal fractures with MR imaging. Radiographics 2003;23(01): 179–187
51 Cicala D, Briganti F, Casale L, et al. Atraumatic vertebral compression fractures: differential diagnosis between benign osteoporotic and malignant fractures by MRI. Musculoskelet Surg 2013;97 (Suppl 2):S169–S179
52 Geith T, Reiser M, Baur-Melnyk A. Differentiation between acute osteoporotic and metastatic vertebral body fractures by imaging. [in German]. Unfallchirurg 2015;118(03):222–229
53 Mauch JT, Carr CM, Cloft H, Diehn FE. Review of the imaging features of benign osteoporotic and malignant vertebral compression fractures. AJNR Am J Neuroradiol 2018;39(09): 1584–1592
54 Wu JS, Goldsmith JD, Horwich PJ, Shetty SK, Hochman MG. Bone and soft-tissue lesions: what factors affect diagnostic yield of image-guided core-needle biopsy? Radiology 2008;248(03): 962–970
55 Virayavanich W, Ringler MD, Chin CT, et al. CT-guided biopsy of bone and soft-tissue lesions: role of on-site immediate cytologic evaluation. J Vasc Interv Radiol 2011;22(07):1024–1030

56 Li Y, Du Y, Luo TY, et al. Factors influencing diagnostic yield of CT-guided percutaneous core needle biopsy for bone lesions. Clin Radiol 2014;69(01):e43–e47
57 Yang SY, Oh E, Kwon JW, Kim HS. Percutaneous image-guided spinal lesion biopsies: factors affecting higher diagnostic yield. AJR Am J Roentgenol 2018;211(05):1068–1074
58 Park SK, Lee IS, Choi JY, et al. CT and MRI of fibrous dysplasia of the spine. Br J Radiol 2012;85(1015):996–1001
59 Zhang Y, Zhang C, Wang S, Wang H, Zhu Y, Hao D. Computed tomography and magnetic resonance imaging manifestations of spinal monostotic fibrous dysplasia. J Clin Imaging Sci 2018;8:23
60 Boudabbous S, Paulin EN, Delattre BMA, Hamard M, Vargas MI. Spinal disorders mimicking infection. Insights Imaging 2021;12 (01):176
61 Ledermann HP, Schweitzer ME, Morrison WB, Carrino JA. MR imaging findings in spinal infections: rules or myths? Radiology 2003;228(02):506–514
62 Braun A, Germann T, Wünnemann F, et al. Impact of MRI, CT, and clinical characteristics on microbial pathogen detection using CT-guided biopsy for suspected spondylodiscitis. J Clin Med 2019;9 (01):32
63 Rehm J, Veith S, Akbar M, Kauczor HU, Weber MA. CT-guided percutaneous spine biopsy in suspected infection or malignancy: a study of 214 patients. Fortschr Röntgenstr 2016;188(12): 1156–1162
64 Spira D, Germann T, Lehner B, et al. CT-guided biopsy in suspected spondylodiscitis—the association of paravertebral inflammation with microbial pathogen detection. PLoS One 2016;11(01): e0146399
65 Bonar SF, Watson G, Gragnaniello C, Seex K, Magnussen J, Earwaker J. Intraosseous hibernoma: characterization of five cases and literature review. Skeletal Radiol 2014;43(07):939–946
66 Kyriakos M. Benign notochordal lesions of the axial skeleton: a review and current appraisal. Skeletal Radiol 2011;40(09): 1141–1152
67 Nishiguchi T, Mochizuki K, Ohsawa M, et al. Differentiating benign notochordal cell tumors from chordomas: radiographic features on MRI, CT, and tomography. AJR Am J Roentgenol 2011;196(03): 644–650
68 Iorgulescu JB, Laufer I, Hameed M, et al. Benign notochordal cell tumors of the spine: natural history of 8 patients with histologically confirmed lesions. Neurosurgery 2013;73(03):411–416
69 Ishida T, Dorfman HD, Steiner GC, Norman A. Cystic angiomatosis of bone with sclerotic changes mimicking osteoblastic metastases. Skeletal Radiol 1994;23(04):247–252
70 Boyse TD, Jacobson JA. Case 45: cystic angiomatosis. Radiology 2002;223(01):164–167
71 Vanhoenacker FM, Schepper AM, Raeve H, Berneman Z. Cystic angiomatosis with splenic involvement: unusual MRI findings. Eur Radiol 2003;13(Suppl 6):L35–L39